Supplementary Information for On the Mechanical Properties and Fracture Patterns of the Nonbenzenoid Carbon Allotrope (Biphenylene Network): A Reactive Molecular Dynamics Study

M. L. Pereira Júnior,[1] W. F. da Cunha,[1] R. T. de Sousa Junior,[2]
G. D. Amvame Nze,[2] D. S. Galvão,[3,4] and L. A. Ribeiro Júnior[1]

[1] *Institute of Physics, University of Brasília, 70.919-970, Brasília, Brazil.*

[2] *Department of Electrical Engineering, University of Brasília 70919-970, Brazil.*

[3] *Applied Physics Department, University of Campinas, Campinas, São Paulo, Brazil.*

[4] *Center for Computing in Engineering and Sciences, University of Campinas, Campinas, São Paulo, Brazil.*

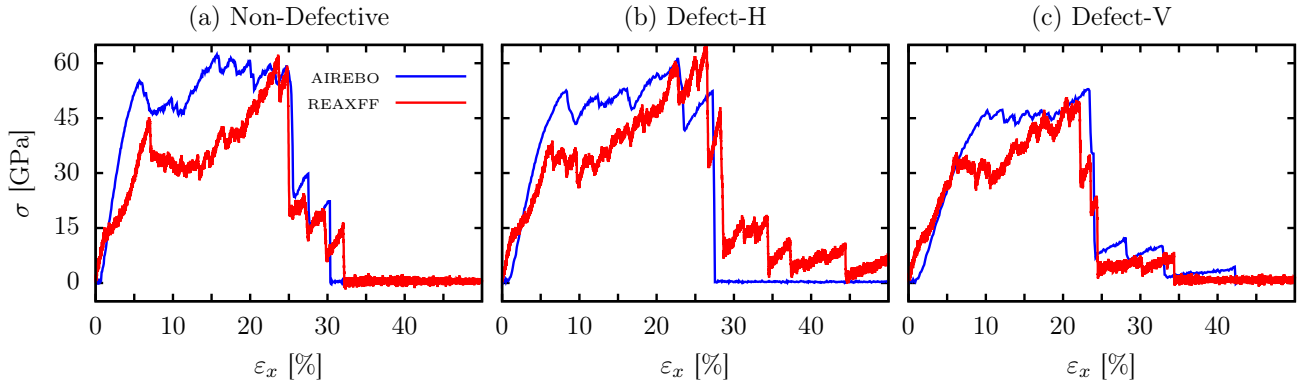

FIG. S1. Stress-strain curves (for strain applied along the x-direction) for: (a) non-defective, (b) horizontally defective (Defect-H), and (c) vertically defective (Defect-V) BPN using AIERBO (blue line) and ReaxFF (red line) potentials. One can note that the stress-strain relationship for the model BPN lattices studied here presents similar behavior for simulations using the AIREBO and ReaxFF potentials.

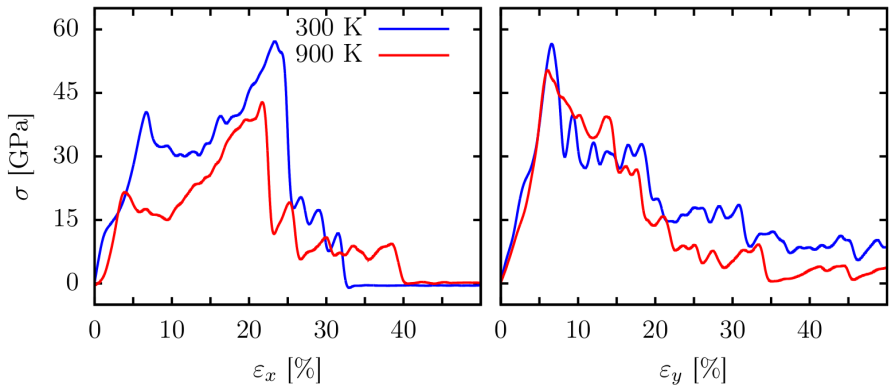

FIG. S2. Stress-strain curves (for strain applied along the x-direction) for the BPN stretching process at 300K and 900K. As expected, the temperature significantly reduces the ultimate stress and the fracture strain values. The reduction in these critical values is related to the increase in the amplitude vibrations, which are imposed by a higher degree of thermal fluctuations when temperature increases. This effect leads to elongations of all C-C bonds followed by several C-C bond-breaking, weakening the monolayer. Note that the first BPN phase transition occurs at 1000K.

Non-Defective				Defective-H				Defective-V			
Potential	Y_M [GPa]	FS [%]	US [GPa]	Potential	Y_M [GPa]	FS [%]	US [GPa]	Potential	Y_M [GPa]	FS [%]	US [GPa]
REAXFF	1019.4	24.9	61.3	REAXFF	986.4	26.6	64.4	REAXFF	760.7	22.3	49.8
AIREBO	1037.4	25.5	61.6	AIREBO	995.1	27 já.4	60.7	AIREBO	747.7	23.6	52.1

TABLE S1. Elastic properties, Young's Modulus (Y_M), Fracture Strain (FS), and Ultimate Strength (US), obtained by fitting the stress-strain curves of the BPN cases investigated here (considering the strain applied along the x-direction). One can conclude that the elastic properties calculated with the AIREBO potential are comparable to their respective values presented in the text using the ReaxFF potential.

300 K						900 K					
σ_x			σ_y			σ_x			σ_y		
Y_M [GPa]	FS [%]	US [GPa]	Y_M [GPa]	FS [%]	US [GPa]	Y_M [GPa]	FS [%]	US [GPa]	Y_M [GPa]	FS [%]	US [GPa]
1019.4	24.9	61.3	745.5	6.7	61.0	829.0	22.6	45.7	572.0	6.2	53.9

TABLE S2. Elastic properties, Young's Modulus Y_M, Fracture Strain (FS), and Ultimate Strength (US), obtained by fitting the stress-strain curves of the BPN stretching at 300K and 900K (considering the strain applied along the x-direction).

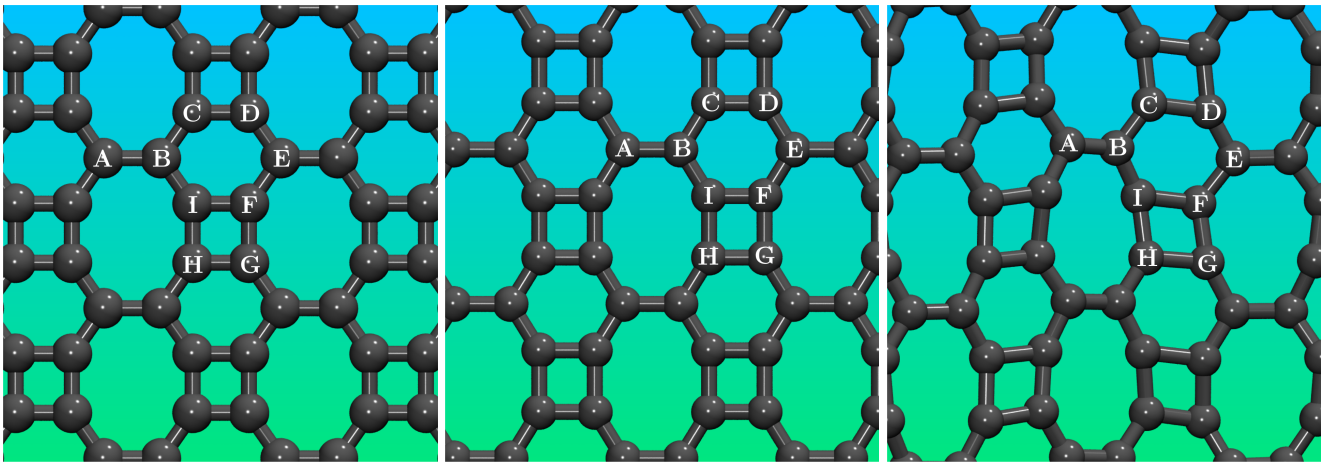

FIG. S3. From left to right: final structures obtained from geometry optimizations using DFT, ReaxFF, and the AIREBO potential. We can see that the AIREBO results differ substantially from the DFT ones, whereas the ReaxFF ones are very similar. The AIREBO structure presents a buckling effect that was not observed in the DFT calculations performed here and in other studies in the literature [1, 2]. Here, the DFT calculations were carried out using the Quantum-Espresso code [3]. Vanderbilt-type ultrasoft pseudopotentials and generalized gradient approximation (GGA) with a Perdew–Burke–Ernzerhof were used for the exchange-correlation. We found that cutoff energy of 544 eV and a $2 \times 2 \times 1$ k-point mesh (generated using the Monkhorst–Pack scheme) were sufficient for the total energy to converge within 0.01 meV/atom.

[1] O. Rahaman, B. Mortazavi, A. Dianat, G. Cuniberti, and T. Rabczuk, Metamorphosis in carbon network: From penta-graphene to biphenylene under uniaxial tension, FlatChem **1**, 65 (2017).
[2] Y. Luo, C. Ren, Y. Xu, J. Yu, S. Wang, and M. Sun, A first principles investigation on the structural, mechanical, electronic, and catalytic properties of biphenylene, Scientific reports **11**, 1 (2021).
[3] P. Giannozzi, S. Baroni, N. Bonini, M. Calandra, R. Car, C. Cavazzoni, D. Ceresoli, G. L. Chiarotti, M. Cococcioni, I. Dabo, *et al.*, Quantum espresso: a modular and open-source software project for quantum simulations of materials, Journal of physics: Condensed matter **21**, 395502 (2009).

Bond	DFT	ReaxFF	Airebo
A–B	1.43 Å	1.43 Å	-
B–C/D–E/E–F/B–I	1.40 Å	1.37 Å	-
C–D/I–F/H–G	1.41 Å	1.39 Å	-
F–G/H–I	1.48 Å	1.54 Å	-

TABLE S3. Calculated bond lengths using DFT and the ReaxFF potential. It is worthwhile to mention that the bond lengths in the optimized lattices obtained using DFT and ReaxFF potential are very similar. The bond lengths from the AIREBO potential were not included here since they vary substantially in the optimized lattice with no correspondence with the results obtained using DFT and ReaxFF potential.

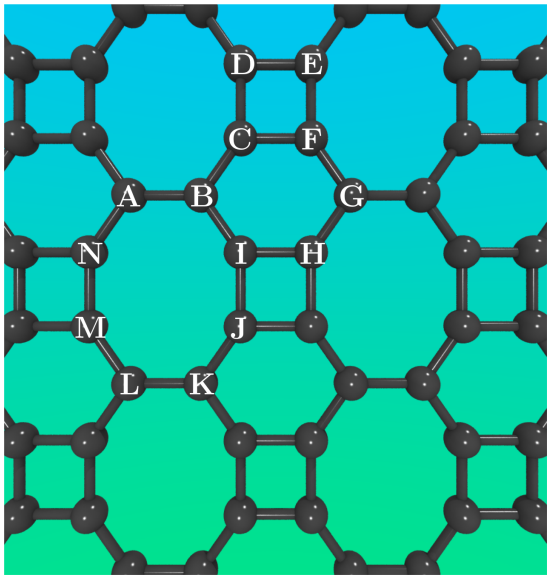

FIG. S4. Atomic indexes used for presenting the angle values in Table S4, according to the three types of rings present in the BPN.

Angle	DFT	ReaxFF	Airebo
AB̂I/JK̂L/KL̂M/NÂB/BĈF/CF̂G/GĤI/HÎB	125°	122°	-
BÎJ/IĴK/LM̂N/MN̂A	145°	148°	-
CD̂E/DÊF/EF̂C/FĈD	90°	90°	-
FĜH/IB̂C	110°	117°	-

TABLE S4. Calculated bond angles using DFT and the ReaxFF potential. It is worthwhile to mention that the bond angles in the optimized lattices obtained using DFT and the ReaxFF potential are very similar. The bond angles from the AIREBO potential were not presented here since they vary substantially in the optimized lattice with no correspondence with the results obtained using DFT and ReaxFF potential.